Anterior cingulate cortex activity regulates effort-based decision making

Abbreviated title: *Anterior cingulate cortex in effortful choice*

Evan E. Hart[1a], Garrett J. Blair[1a], Thomas J. O'Dell[2-4], Hugh T. Blair[1-3b], and Alicia Izquierdo*[1-3,5b]

[1]Department of Psychology, UCLA, Los Angeles, CA 90095 USA
[2]The Brain Research Institute, UCLA, Los Angeles, CA 90095 USA
[3]Integrative Center for Learning and Memory, UCLA, Los Angeles, CA 90095 USA
[4]Department of Physiology, UCLA, Los Angeles, CA 90095 USA
[5]Integrative Center for Addictions, UCLA, Los Angeles, CA, 90095 USA

[a]EEH and GJB, co-first authors. These authors contributed equally to this work
[b]HTB and AI, co-senior authors.

Author contributions: EEH, GJB, and AI designed the research; EEH, GJB, and TJO performed the research; EEH, GJB, HTB, TJO, and AI analyzed data; EEH, GJB, TJO, HTB, and AI wrote the paper.

Correspondence: *Alicia Izquierdo, Ph.D. email: aizquie@psych.ucla.edu Ph: +1 310 825 3459

Manuscript Information:

Pages	40
Figures	7
Supp	3
Tables	0

Words: Abstract 150/150
Character count: 37,005 (excluding methods)

Abstract (150 words)

Prior evidence suggests that the anterior cingulate cortex (ACC) is required for choosing high effort options over less effortful alternatives. Here, rats earned a high-value sucrose reward by lever pressing on a progressive ratio schedule in either the presence (choice) or absence (no-choice) of freely available, low-value lab chow. Disruption of ACC, either via chemogenetic inhibition or excitation, reduced lever pressing for high-value reward in the choice, but not in the no-choice, condition. In vivo calcium imaging revealed cell populations in ACC that selectively responded prior to lever pressing and during sucrose retrieval. These responses were significantly weaker during choice than no-choice sessions, which may have rendered them more susceptible to chemogenetic disruption. Our results suggest that neural responses in ACC encode the relative value of competing outcomes, and that the amount of effort an animal is willing to exert is proportional to the magnitude of this relative value signal.

Keywords: *prefrontal cortex, amygdala, orbitofrontal cortex, DREADDs, miniscopes, single-photon, calcium imaging*

Introduction

Real-world decisions rarely involve choosing between unambiguously favorable vs. unfavorable options. Often, options must be evaluated along multiple dimensions that incorporate an evaluation of the rewards themselves as well as the actions or efforts to procure them (Skvortsova et al., 2014). For example, we typically make decisions between options in comparison, where one outcome may be more costly (i.e. more effortful) yet more preferred than the other.

Outside of the striatum, which has been the major region of study in such effort-based decision making studies (Cousins et al., 1996; Ghods-Sharifi and Floresco, 2010; Nowend et al., 2001; Salamone et al., 2007; Salamone et al., 2003; Salamone et al., 1994; Salamone et al., 1991), the anterior cingulate cortex (ACC) is also involved in the evaluation of both physical and cognitive effort costs (Cowen et al., 2012; Floresco and Ghods-Sharifi, 2007; Hillman and Bilkey, 2010, 2012; Hosking et al., 2014; Schweimer and Hauber, 2005; Walton et al., 2003; Winstanley and Floresco, 2016). Neurons in both rat and primate ACC signal value during economic decision-making (Azab and Hayden, 2017; Hunt and Hayden, 2017; Lapish et al., 2008; Mashhoori et al., 2018). Neural responses in this region also track trial-by-trial outcomes of choices (Akam et al., 2017; Procyk et al., 2000; Seo and Lee, 2007; Shidara and Richmond, 2002), reward history (Bernacchia et al., 2011), reward prediction errors, (Hayden et al., 2009; Hyman et al., 2017; Kennerley et al., 2011), and counterfactual options (‘rewards not taken’) (Hayden et al., 2009; Mashhoori et al., 2018). Indeed, both anatomical and functional evidence supports the idea that ACC activity supports representations of reward value and action outcomes (Heilbronner and Hayden, 2016; Shenhav et al., 2013).

In rats, effort t-maze and effort discounting tasks typically require the animal to select among different magnitudes of the same reward identity (i.e. more sucrose pellets vs. fewer sucrose pellets). However, a paradigm that involves selecting between qualitatively different reinforcers may also closely model human decisions where we encounter options that are more/less preferred, not more/less of the same reward identity (Cousins and Salamone, 1994; Nowend et al., 2001; Nunes et al., 2013; Randall et al., 2014a; Randall et al., 2015; Randall et al., 2012; Salamone et al., 2007; Salamone et al., 2017; Salamone et al., 1991; Yohn et al., 2016a; Yohn et al., 2016b; Yohn et al., 2016c). The majority of the seminal rodent studies probing ACC in effort-based choice (Floresco and Ghods-Sharifi, 2007; Hauber and Sommer, 2009; Walton et al., 2003; Walton et al., 2002; Winstanley and Floresco, 2016) have used traditional pharmacological, lesion, and electrophysiological approaches, so a fine-grained analysis involving viral-mediated targeting of ACC in effort choice has not yet been reported.

Here, we tested the effects of inhibitory (hM4Di, or G_i) and excitatory (hM3Dq, or G_q) Designer Receptors Exclusively Activated by Designer Drugs (DREADDs) in ACC on the same effortful choice task that we previously probed following lesions (Hart et al., 2017) and pharmacological inactivations (Hart and Izquierdo, 2017). Briefly, our task required rats to choose between working for a preferred reward (sucrose) vs. consuming a concurrently and freely-available, but less preferred reward (standard chow). We assessed the role of ACC on (i) progressive ratio (PR) lever pressing for sucrose pellets (i.e. general motivation), and (ii) PR lever pressing with choice (PRC) of a freely-available alternative (i.e. effortful decision-making: choosing between working for sucrose pellets vs. concurrently available laboratory chow). We also tested the effects of ACC inhibition and excitation on the choice between sucrose pellets vs. chow when these reinforcers were both freely available (i.e. “free choice”). Finally, in a separate

cohort of animals we utilized *in vivo* miniaturized fluorescence microscopy (UCLA "miniscopes") to compare calcium activity in ACC and to evaluate how populations of neurons in this region respond during no-choice (PR) and choice (PRC) sessions.

Results

Histology. Reconstructions of viral spread confirmed that most placements were centered on the targeted region of Cg1 in ACC (**Figure 1**). DREADD expression was driven by a CaMKIIα promoter, which is thought to selectively target projection neurons in cortex (Nathanson et al., 2009; Wang et al., 2013). Viral spread in the G_i and G_q groups was quantified by pixel count using GIMP software (see Methods). There was no significant difference between G_i and G_q groups ($t_{(20)}$=2.03 p=0.056; G_i = 25258 ± 3121 total mean pixels; G_q = 17736 ± 2002 total mean pixels).

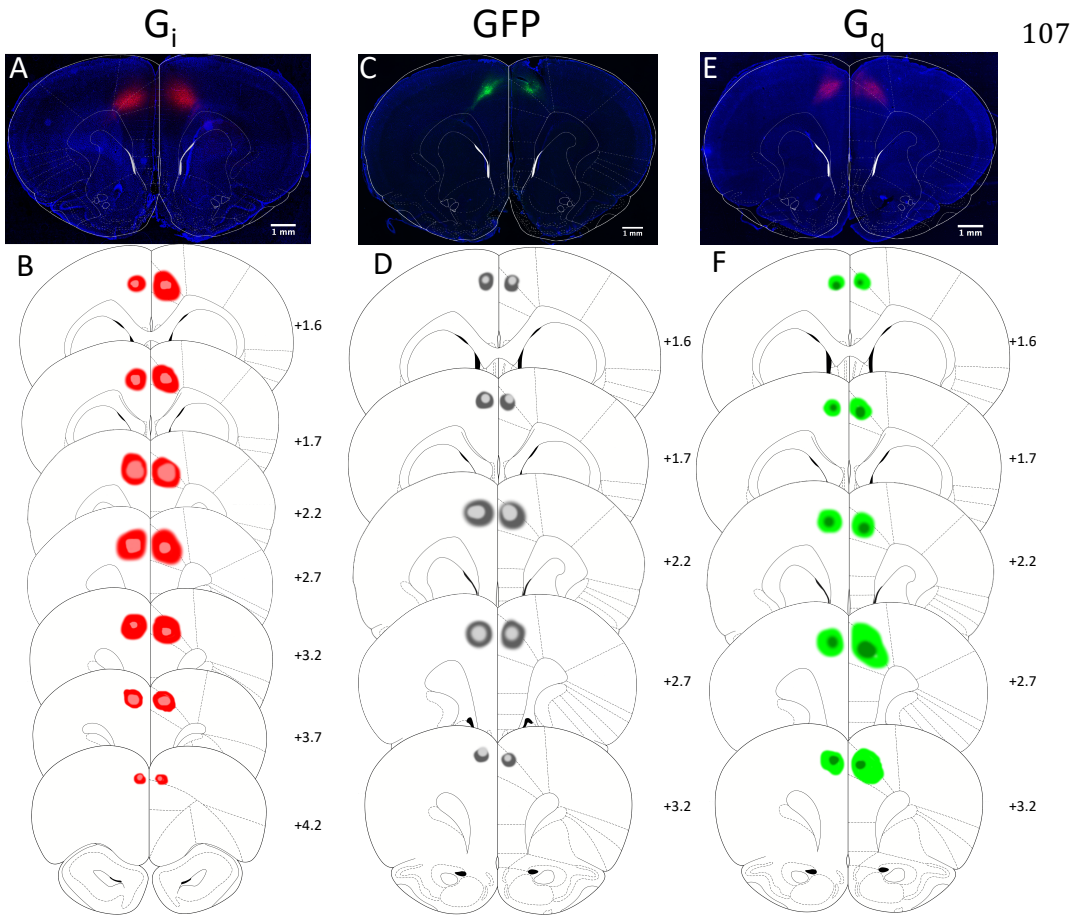

Figure 1. Expression of inhibitory and excitatory DREADDs and null virus eGFP in Anterior Cingulate Cortex. (A) Representative photomicrograph showing hM4Di-mCherry DREADDs under CaMKIIα in ACC, labeled G_i. **(B)** Schematic reconstruction of maximum (red) and minimum (pink) viral spread for all rats. Numerals depict +Anterior-Posterior (AP) level relative to Bregma. Scale bars 1mm. **(C)** Representative photomicrograph showing eGFP (null virus) under CaMKIIα in ACC, labeled GFP. **(D)** Schematic reconstruction of maximum (dark grey) and minimum (light grey) viral spread for all rats. Numerals depict +Anterior-Posterior (AP) level relative to Bregma. Scale bars 1mm. **(E)** Representative photomicrograph showing hM3Dq-mCherry DREADDs expression in ACC, labeled G_q. **(F)** Schematic reconstruction of maximum (light green) and minimum (dark green) viral spread for all rats. Numerals depict +Anterior-Posterior (AP) level relative to Bregma. Scale bars 1mm.

Ex vivo electrophysiological validation of DREADDs. We confirmed the efficacy of our DREADDs in slice recordings. A separate group of rats was prepared with G_q DREADDs in ACC (Cg1) using identical surgical procedures to the main experiments (**Figure 2A**). As described in Methods, a bipolar stimulating electrode was placed near the medial wall in layer I of ACC, and a glass microelectrode filled with ACSF (resistance = 5–10 MΩ) was placed in layer 2/3 of ACC to record field potentials and multiunit responses elicited by layer 1 stimulation. Using similar methods, we have previously reported that application of CNO strongly suppressed evoked field potentials in G_i transfected slices in ACC (Stolyarova et al., 2019). Here, we found that application of CNO induced spontaneous bursting in four out of six G_q transfected slices (spontaneous activity rate was increased from 0 to 0.06 Hz ± 0.01 Hz, inter-burst intervals were 18.3 ± 2.6 seconds (mean ± SEM, range: 12.4 – 31.6 seconds, n=4 slices from 3 rats) (**Figure 2B**). In two other G_q transfected slices where no spontaneous bursting was observed, CNO application reduced threshold for stimulation induced postsynaptic responses (n=2 slices from 3 rats), with a sharp transition from

no response to maximal response as a function of stimulation intensity (**Figure 2C**). CNO had no effect on responses in non-transfected slices (n=3 slices from 3 rats) (**Figure 2D**).

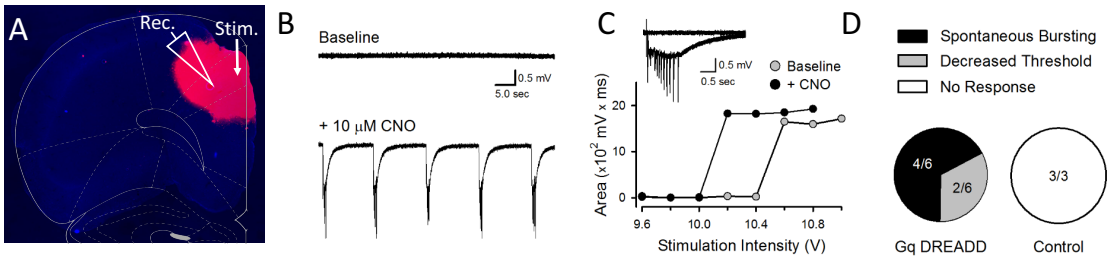

Figure 2. Excitatory hM3Dq DREADDs validation in Anterior Cingulate Cortex. Electrophysiological effect of bath application of CNO in slice. **(A)** Representative photomicrograph showing hM3Dq-mCherry DREADDs under CaMKIIα in a recording site of a 400 µm slice in ACC. **(B)** Spontaneous ACC activity in a G_q DREADD-expressing slice before (top) and after 20 min bath application of 10 µM CNO (bottom). CNO-induced spontaneous bursting was seen in 4 out of 6 G_q DREADD-expressing slices from 3 rats. **(C)** In the two G_q DREADD-expressing slices that failed to show spontaneous bursting there was a decrease in the threshold for stimulation induced postsynaptic responses. Plot shows results from one of these slices before (baseline) and after CNO application. **(D)** Summary of responses to CNO in G_q DREADD-expressing and control slices. CNO did not elicit either spontaneous bursting or decrease threshold for evoked responses in all 3 of the control (non-transfected) slices from 3 rats.

Lever press training. Rats were trained over a series of days to press a lever for food on a progressive ratio (PR) schedule (where the required number of presses to earn each pellet increased throughout the session according to a prescribed formula; see Methods). After reaching criterion, rats received systemic injections of either VEH or CNO (in a counterbalanced repeated measures design) prior to subsequent sessions, which alternated between two different types: 1) progressive ratio choice (PRC) sessions during which a ceramic ramekin containing 18 g of freely available lab chow was introduced to the chamber (modified from Randall et al., 2012), and 2) PR only sessions during which the rat pressed on the progressive ratio schedule with no other food available (as during prior training). During PRC sessions, rats were free to choose between consuming freely-available (but less preferred) chow versus lever pressing for preferred sucrose pellets,

157 whereas during PR sessions, the only reward option was to lever press for sucrose pellets. In
158 general, lever pressing rates were higher during PR sessions than PRC sessions (**Figures 3 and 4**),
159 indicating the free chow draws behavior away from lever pressing (Salamone et al., 2018) and
160 animals emit fewer lever presses in PRC sessions than in PR sessions.

161 *G_i inhibition of ACC.* We found that chemogenetic inhibition of ACC significantly
162 decreased lever pressing during PRC but not PR sessions. A paired-samples t-test revealed CNO
163 significantly reduced the total mean number of lever presses during 30 min PRC sessions
164 ($t_{(10)}$=3.047 p=0.01; VEH = 216.1 ± 52.85 presses; CNO = 173.2 ± 40.27 presses) **(Figure 3A)**.
165 The total amount of chow consumed during 30 min PRC sessions was not affected by CNO
166 treatment ($t_{(10)}$=1.048 p=0.32; VEH = 7.79 ± 0.33 g; CNO = 7.50 ± 0.36 g) **(Figure 3B)**. CNO had
167 no effect on PR responding in the absence of freely available chow ($t_{(10)}$=0.26 p=0.80; VEH =
168 905.1 ± 102.00 presses; CNO = 893.9 ± 128.3 presses) **(Figure 3C)**. A two-way ANOVA (food
169 type- sucrose, chow; injection- VEH, CNO) on the amount of sucrose and chow consumed during
170 free choice testing revealed a significant main effect of food type ($F_{(1,10)}$=12.02 p=0.006; sucrose
171 = 8.59 ± 0.83 g; chow = 4.19 ± 0.34 g), but no significant food type by injection interaction
172 ($F_{(1,10)}$=1.415 p=0.26), or main effect of injection ($F_{(1,10)}$=0.01 p=0.91) was found **(Supplementary**
173 **Figure 1A)**. Hence, food preference was intact and not affected by CNO injection.

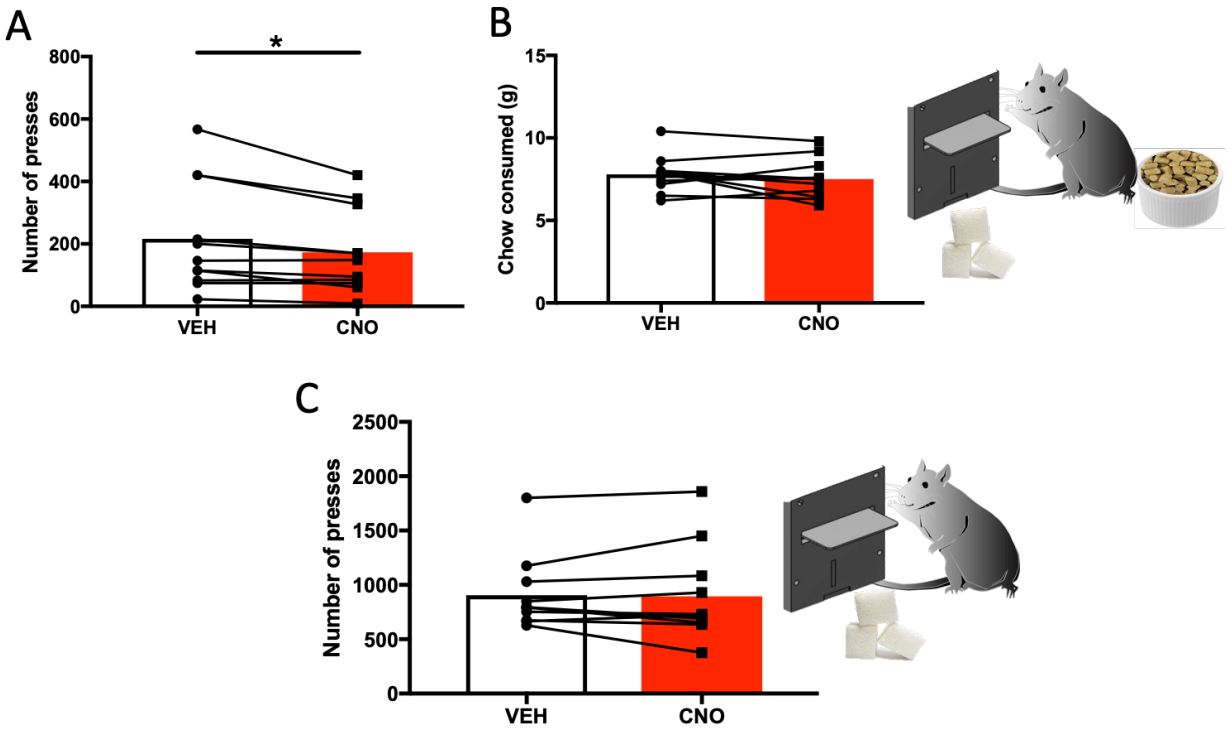

Figure 3. Effects on choice behavior following DREADDs inhibition of Anterior Cingulate Cortex. (A) Mean lever presses during PRC sessions, when rats were presented with both the possibility of lever pressing under a PR schedule for sucrose pellets and freely-available chow. Shown is within-subject, counterbalanced choice behavior under vehicle and CNO. CNO significantly reduced the number of lever presses in this condition. **(B)** Total chow consumed during choice testing was not different between vehicle and CNO conditions. **(C)** Mean lever presses during PR sessions when there was no chow available as an alternative option. Lever pressing was not different between vehicle and CNO conditions. * $p<0.05$.

G_q excitation of ACC. Similar to results for the G_i experiment, we found that chemogenetic excitation of ACC significantly decreased lever pressing during PRC but not PR sessions. Using identical procedures to the inhibition experiment, a separate group of rats was assessed on effortful choice following excitatory G_q DREADDs transfection in ACC. A paired-samples t-test revealed CNO significantly reduced the total mean number of lever presses during 30 min PRC sessions ($t_{(10)}$=2.31 p=0.04; VEH = 210.7 ± 49.44 presses; CNO = 166.6 ± 40.4 presses) **(Figure 4A)**. The total amount of chow consumed during 30 min PRC sessions was not affected by CNO treatment

($t_{(10)}$=0.39 p=0.71; VEH = 7.71 ± 0.36 g; CNO = 7.81 ± 0.42 g) **(Figure 4B)**. CNO had no effect on PR responding in the absence of freely available chow ($t_{(10)}$=1.15 p=0.28; VEH = 1107.00 ± 99.66 presses; CNO = 1209.00 ± 156.3 presses) **(Figure 4C)**. A two-way ANOVA (food type- sucrose, chow; injection- VEH, CNO) on the amount of sucrose and chow consumed during free choice testing revealed a significant main effect of food type ($F_{(1,10)}$=47.63 p<0.001; sucrose = 9.68 ± 0.47 g; chow = 5.10 ± 0.37 g), but no significant food type by injection interaction ($F_{(1,10)}$=2.27 p=0.16) or main effect of injection ($F_{(1,10)}$=0.06 p=0.81), indicating food preference was intact and unaffected by CNO **(Supplementary Figure 1B)**.

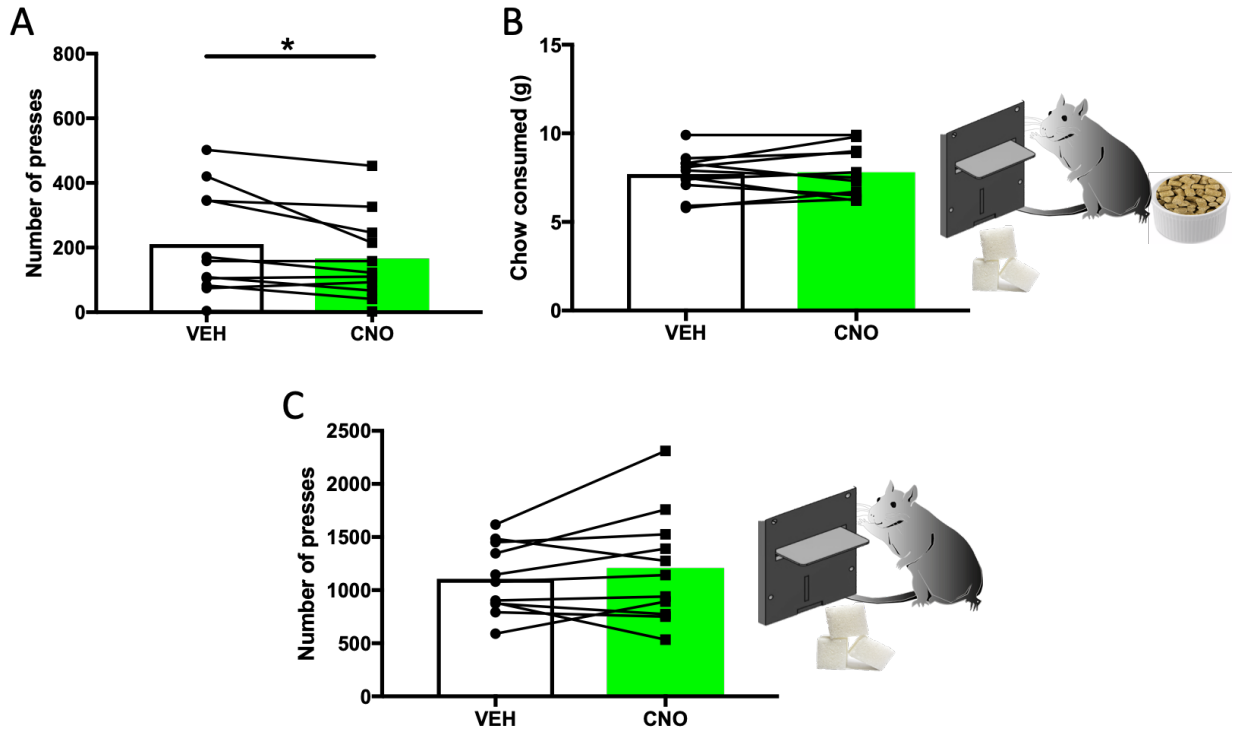

Figure 4. Effects on choice behavior following DREADDs stimulation of Anterior Cingulate Cortex. (A) Mean lever presses during PR sessions, when rats were presented with both the possibility of lever pressing under a PR schedule for sucrose pellets and freely-available chow. Shown is within-subject, counterbalanced choice behavior under vehicle and CNO. CNO significantly reduced the number of lever presses in this condition. **(B)** Total chow consumed during choice testing was not different between vehicle and CNO conditions. **(C)** Mean lever presses during PR sessions when there was no chow available as an alternative option. Lever pressing was not different between vehicle and CNO conditions. * p<0.05.

GFP (null virus) control. To test whether results for Gi and Gq DREADDs could be explained by virus exposure alone, a control virus carrying only GFP (but no DREADD receptors) was infused into ACC in a separate group of rats. A paired t-test revealed no effect of CNO on the total mean number of lever presses during 30 min PRC sessions ($t_{(9)}$=0.48 p=0.64; VEH = 314.9 ± 57.34 presses; CNO = 302.7 ± 59.66 presses) **(Supplementary Figure 2A)**. The total amount of chow consumed during 30 min PRC sessions was not affected by CNO treatment ($t_{(9)}$=0.26 p=0.80; VEH = 6.65 ± 0.99 g; CNO = 6.85 ± 0.34 g) **(Supplementary Figure 2B)**. CNO also had no effect on PR responding in the absence of freely available chow ($t_{(10)}$=0.73 p=0.48; VEH = 1001.00 ± 109.4 presses; CNO = 1043.00 ± 120.00 presses) **(Supplementary Figure 2C)**. A two-way ANOVA (food type- sucrose, chow; injection- VEH, CNO) on the amount of sucrose and chow consumed during free choice testing revealed a significant main effect of food type ($F_{(1,9)}$=80.63 p<0.001; sucrose = 8.37 ± 0.60 g; chow = 3.19 ± 0.35 g), indicating food preference was intact. No significant food type by injection interaction ($F_{(1,9)}$=1.27 p=0.29), or effect of injection ($F_{(1,9)}$=0.97 p=0.35) was found **(Supplementary Figure 1C)**.

Calcium imaging in rat ACC. A group of 4 rats received infusions of AAV9- CaMKIIα-GCaMP6f and was subsequently implanted with 1.8 mm diameter 0.25 pitch GRIN lenses in Cg1 (**Figure 5**). Rats were then trained on lever pressing and tested during PR and PRC sessions identical to those described above for DREADD experiments. GRIN lens implanted rats were also given "satiety control" (CON) sessions, where rats were pre-fed with chow in the operant chamber, and then were allowed to lever press on a PR schedule in the absence of chow. This was to control for the possibility that neural encoding could be influenced by satiety from chow consumption, regardless of whether chow was freely available during the lever pressing task.

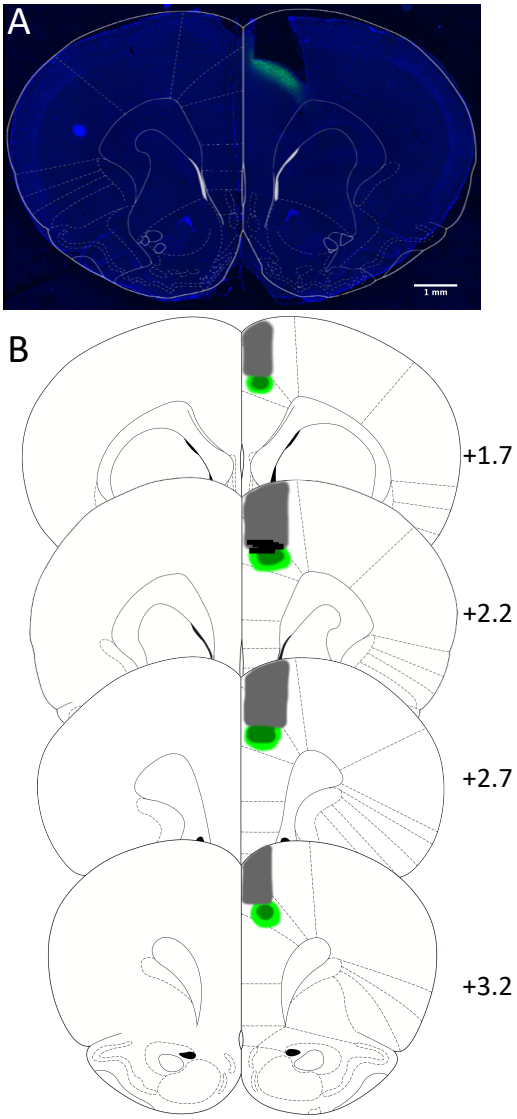

Figure 5. Calcium imaging histology in Anterior Cingulate Cortex. (A) Representative photomicrograph showing GCaMP6f expression and aspiration site for lens placement for ACC imaging. (**B**) Schematic reconstruction of maximum (light green), minimum (dark green) viral spread, and maximum aspiration damage (gray). Black bars represent ACC recording sites. Numerals depict +Anterior-Posterior (AP) level relative to Bregma. Scale bar 1mm.

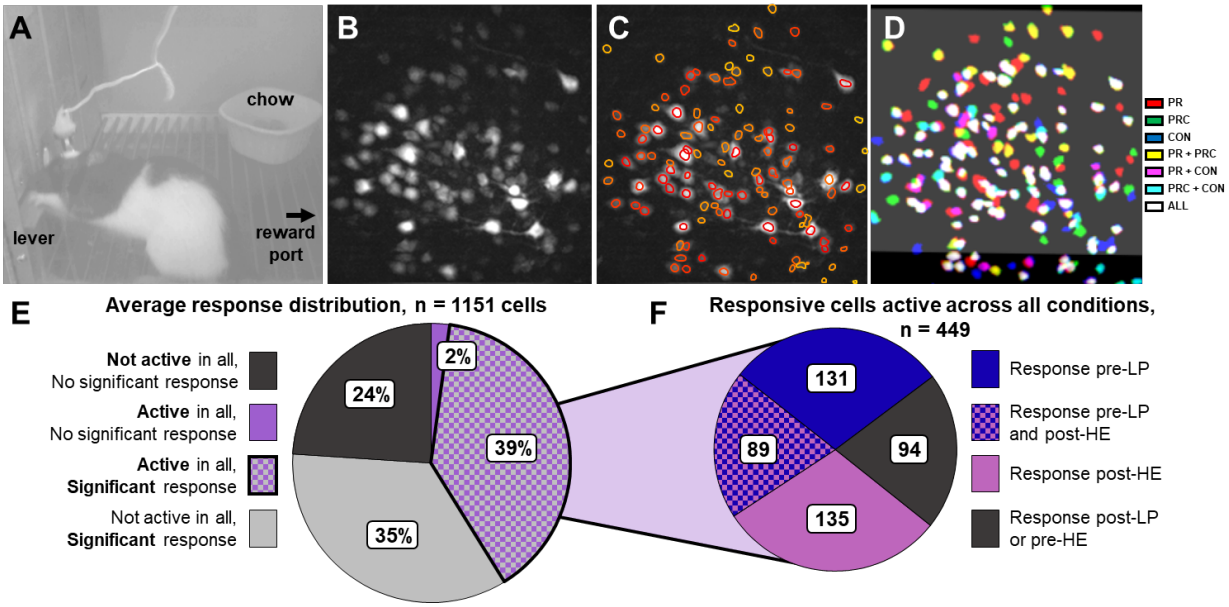

Figure 6. **Anterior Cingulate Cortex calcium imaging. (A)** Example of PRC behavior session with the miniscope on the rat's head; both sucrose and chow options are available, with reward port on the right (just out of view) and chow in the ramekin. **(B)** Maximum projection image of calcium fluorescence from the session in 'A' after motion correction and neural enhancement. **(C)** Same as in 'B' with extracted cell contours overlaid. **(D)** Cell contours matched across three recording sessions (one of each type: PR, PRC, CON); color codes indicate the subset of sessions during which a given cell fired at least one spike. **(E)** Distribution of response properties for all recorded cells (1151 cells from 4 rats). 39% (449) of the total unique 1151 cells were active in at least one of each session type and significantly modulated by behavior. These cells were further analyzed (see Figure 7). **(F)** Further classification of 449 cells that were active in at least one session of each type (PR, PRC, and CON) and had a significant response to either lever press (LP) or reward port head entry (HE) events during at least one session type; We separately analyzed cells which responded before lever-press (pre-LP) and after head-entry (post-HE).

Single cell responses. We recorded a total of 1151 neurons from ACC in 4 animals (136 from rat #1, 567 from rat #2, 254 from rat #3, 194 from rat #4). Each neuron's spike events were extracted by deconvolving its denoised calcium trace (sampling rate = 7.5 Hz; see Methods). A cell's baseline spiking probability was measured during time periods that were at least ±5 s away from any lever press ("LP") or head entry ("HE") into the reward magazine. To analyze neural responses to LP and HE events, perievent time histograms (PETHs) were generated by combining

data from all sessions of a given type (PR, PRC, or CON) during which the cell fired at least one spike. Spike probabilities were computed in time bins within ±3 s of the trigger event (LP or HE), and compared against baseline using a binomial probability test (bin width = 133.33 ms, derived from the 7.5 Hz frame rate). Any cell exhibiting at least 3 bins with spike rate exceeding baseline at the $p<.01$ level was classified as "responsive" within the 6 s period surrounding the trigger event.

To analyze how responses to HP and LE events varied with session type (PR, PRC, CON), we identified a subset of 449 neurons (39% of all recorded cells) that were: 1) active during at least one session of each type, and 2) significantly responsive to either LP or HE events (or both) during at least one of the three session types (**Figure 6E**). The natural sequence of task behavior caused LP events to often be followed within 3 s by HE events, and likewise, for HE events to often be preceded within 3 s by LP events (**Supplementary Figure 3**). This was because immediately after completing the required number of LPs for a trial, the lever was retracted and the rat went to the magazine where it generated an HE event that closely followed the last LPs of that trial. Consequently, cells that responded after LP events or before HE events could not be unambiguously classified as responsive to one kind of event or the other (LPs versus HEs, because the response was proximal to both kinds of events). By contrast, LP events were rarely preceded within 3 s by HE events, and HE events were rarely followed within 3 s by LP events (**Supplementary Figure 3**). We thus restricted further analysis to cells that consistently responded before but not after LP events ("pre-LP" cells, n=131), or after but not before HE events ("post-HE" cells, n=135), or both ("LP-HE" cells, n=89); cells that responded after LP events or before HE events (n=94) were omitted from further analysis (**Figure 6F**).

Population responses preceding LP events. For every cell that responded prior to LP events (that is, cells belonging to either the pre-LP or LP-HE cell populations), three LP-triggered PETHs

were generated (one for each session type: PR, PRC, CON; **Figure 7A**). To normalize the response of each cell, the bins of all three PETHs for the cell were divided by the maximum value observed in any bin across all three PETHs. A population average of responses surrounding LP events was computed as the mean of the normalized PETHs (**Figure 7B**). Each cell's summed normalized response during the 3 s preceding LP events was computed for each session type, and it was found that pre-LP responses differed significantly by session type (Friedman's non-parametric ANOVA: p = 8.57e-10; **Figure 7B,C**). Post-hoc comparisons revealed that the pre-LP response was greatest during PR sessions, smallest during PRC sessions, and intermediate during CON sessions, with significant differences between all three session types (Sign rank test: PR > CON, p = 7.94e-04; PR > PRC, p = 3.22e-12; CON > PRC, p = 4.14e-06) (**Figure 7C**).

Population responses following HE events. For every cell that responded after HE events (that is, cells belonging to either the post-HE or LP-HE cell populations), three HE-triggered PETHs were generated (one for each session type: PR, PRC, CON; **Figure 7D**). Population averaged responses surrounding HE events were computed for each of the three session types, using the same methods described above for LP-triggered PETHs (**Figure 7E**). It was found that post-HE responses different significantly by session type (Friedman's non-parametric ANOVA: p = 6.38e-04; **Figure 7E,F**), and post-hoc comparisons revealed that population responses during PR and CON sessions were not significantly different from one another (Sign rank test: PR = CON, p = 0.22), whereas PRC sessions showed a significantly lower post-HE response than either of the other two session types (Sign rank test: PR > PRC, p = 4.23e-05 ; CON > PRC, p = 1.47e-05). This pattern of results suggests that responses of ACC neurons to rewarding outcomes may depend upon the availability of alternative outcomes (see Discussion).

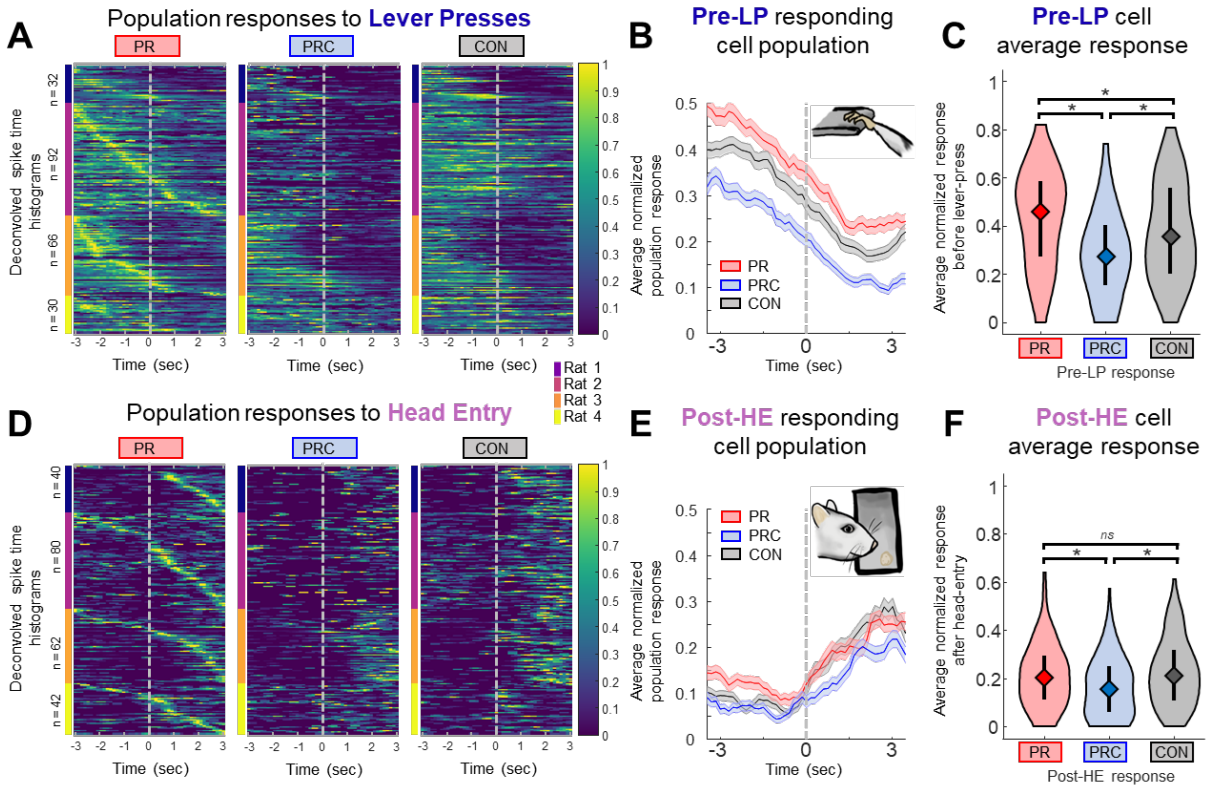

Figure 7. Analysis of Anterior Cingulate Cortex lever press and magazine head entry responsive cells during different session types. (A) Heat plots show normalized PETHs of spike responses for cells classified as "pre-LP" cells. PETHs are sorted first by animal (color code at left) and then by the time bin of their peak activity bin in PR sessions. Cells are matched across session types. **(B)** Mean population response for PR, PRC, and CON sessions; shaded portion denotes 1 standard error. Pre-LP responsiveness was weakest during PRC testing. **(C)** Violin plots of the population activity averaged over the 3 s before lever press. Diamonds mark the median, and lines mark the inner quartiles. Pre-LP responsiveness was weakest during PRC testing. **(D)** Normalized PETHs for cells classified "post-HE" cells. **(E)** Mean population response to HE in PR, PRC, and CON conditions. Post-HE responsiveness was weakest during PRC testing. **(F)** Violin plots for post-HE population activity after HE. Post-HE responsiveness was weakest during PRC testing. *p<.001, *n.s.* not significant.

Discussion

We found that either chemogenetic silencing *or* stimulation of ACC excitatory neurons resulted in decreased PR lever pressing for a qualitatively preferred option, but this effect was only observed when a concurrently available, lower effort alternative was available, and not when lever pressing was the only response option. Chemogenetic manipulations had no effects on the ability to lever

press for sucrose or on food preference. CNO administration also had no effects in rats lacking active DREADD (hM4D-G_i or hM3D-G_q) receptors. Slice electrophysiology confirmed robust inhibition (Stolyarova et al., 2019) and excitation in hM4D-G_i and hM3D-G_q transfected slices, respectively. Finally, we found that ACC calcium activity was modulated by the availability of alternative choice options, in a manner suggesting that ACC neurons may encode the relative value of available reward options (see below). Taken together, these findings support a causal role for ACC in the evaluation of effortful behavior, consistent with recent evidence from single-unit recordings suggesting involvement of this region in "biasing decision-making towards behaviors with highest utility" (Porter et al., 2019).

ACC chemogenetic silencing. The earliest studies probing rat ACC in effort-based choice made use of T-maze tasks where rats selected between the same food option but of different magnitudes (Schweimer and Hauber, 2006; Walton et al., 2003; Walton et al., 2002). The first test of rat ACC in a task where rats chose between qualitatively different options produced negative results (Schweimer and Hauber, 2005); it is possible this was due to pre-training lesions as well as prior behavioral testing, as later work from our lab found that excitotoxic lesions of ACC resulted in decreased PR lever pressing in the context of choice (Hart et al., 2017).

Here, hM3Dq and hM4Di receptors were expressed under a CaMKIIα promoter, thus targeting primarily excitatory pyramidal neurons (Nathanson et al., 2009; Wang et al., 2013), in contrast with prior studies using lesions or inactivations that silence all neural activity. It seems likely that ACC exerts its effects on choice behavior via projections to downstream targets, the densest of which are to dorsal striatum and mediodorsal thalamus (Vogt and Paxinos, 2014), though ACC also sends sparser efferents to ventral striatum and amygdala (Gabbott et al., 2005). A recent report demonstrated a role for dorsal striatal dopamine in effort-based choice (Bailey et

al., 2018). Interestingly, the role of dorsal striatum in effort-based choice is relatively understudied and could be a ripe avenue for future study given the strong cortical afferentation from ACC.

Though reliable, the magnitude of effect observed here with DREADDs was considerably smaller than what we previously observed following lesions (Cohen's d=1.39 lesions vs d=0.28 G_i vs d=0.29 G_q) (Hart et al., 2017), and also smaller than effects we have previously reported from our lab following pharmacological inactivation (Hart and Izquierdo, 2017; 2019) and drug exposure (Hart et al., 2018; Thompson et al., 2017). The smaller effect obtained with DREADDs could be due to several factors. First, unlike NMDA lesions which cause widespread destruction of ACC neurons, DREADD receptors targeted only cells that recognize the CaMKIIα promoter (presumably excitatory projection neurons), and these cells may only have been partially transfected with DREADD receptors. Second, although slice experiments have shown that inhibitory DREADD receptors suppress neural activity in ACC (Stolyarova et al., 2019), and that excitatory DREADDs reliably altered firing patterns of ACC neurons (**Figure 2**), DREADD-induced changes in neural activity may have weaker effects upon behavior than complete pharmacological inactivation of ACC with muscimol, or widespread changes in neural activity following chronic psychostimulant exposure (Hart et al., 2018).

ACC calcium imaging. We used *in vivo* calcium imaging to investigate how ACC neurons responded during lever pressing and reward retrieval (i.e., reward port head entry) during PR, PRC, and CON sessions (**Figure 7**). A total of 449 neurons from 4 rats were successfully recorded during at least one session of each type and had a significant response to surrounding lever press or head entry. About half of these neurons (220/449) fired significantly above baseline during the 3s time window preceding lever presses in at least one of the three session types (**Figure 7A-C**). These pre-lever responses were significantly lower during CON than PR sessions, and since rats were

sated on chow before lever pressing during CON but not PR sessions, it appears that satiety from chow consumption may have attenuated neural responses during the pre-lever period. Consistent with this interpretation, calcium activity during the pre-lever period was also lower during PRC than PR sessions. However, pre-lever activity was even lower during PRC than CON sessions (despite the fact that rats were similarly sated on chow at the start of both PRC and CON sessions), suggesting that satiety on chow plus free chow availability attenuated pre-lever calcium activity even more than satiety alone.

About half of the recorded ACC neurons (224/449) fired significantly above baseline during the 3s time window following head entry into the reward magazine, which was the period during which the rat retrieved and consumed the high value sucrose reward (**Figure 7D-F**). These sucrose responses were similar in magnitude during CON and PR sessions, indicating that satiety from prior chow consumption had little effect on ACC responses to sucrose. By contrast, sucrose-related activity was significantly lower during PRC sessions than during PR and CON sessions, indicating that independently of satiety state, free chow availability attenuated sucrose responses of ACC neurons below the levels seen when sucrose was earned in the absence of free chow.

These findings suggest that the activity of ACC neurons during sucrose consumption encodes the difference between the value of the sucrose versus the value of other available reward options. If no other options are available (as during PR and CON sessions), then the value of other options is zero, and thus nothing is subtracted from the value of the sucrose reward. But if a lower value reward option (such as lab chow during PRC sessions) is available while the rat is working for sucrose, then the nonzero value of the other option may be subtracted from the value of the sucrose reward, reducing the magnitude of ACC responses during sucrose delivery. If this relative value signal for sucrose in ACC is involved in driving motivated effort to work for sucrose, then

398 it would be expected that the rat should exert less effort for sucrose under conditions where the
399 ACC responses to sucrose are smaller. This is exactly what we observed: sucrose responses of
400 ACC neurons were lower during PRC sessions (where lab chow was available as a competing
401 reward option) than during PR or CON sessons (where sucrose was the only reward option). The
402 reduced motivation to lever press might account in part for the attenuated calcium activity we
403 observed in ACC during the pre-lever period of PRC sessions, compared with PR and CON
404 sessions. However, since pre-lever calcium activity was also lower during CON sessions than PR
405 sessions, satiety may have also attenuated calcium activity prior to lever pressing.

406 In summary, neural activity associated with sucrose pellet collection in ACC may be
407 strongest when sucrose is the only available option, and weakened by the presence of the
408 counterfactual choice. This is consistent with prior evidence that rat ACC encodes "the utility of
409 remote locations" that contain rewards not chosen (Mashhoori et al., 2018), and also with findings
410 that nonhuman primate dorsal ACC is involved in actively signaling the value of leaving a patch
411 in pursuit of another option in foraging tasks (Hayden et al., 2011). Dorsal ACC also signals the
412 value of the rejected (counterfactual) option (Blanchard and Hayden, 2014), which is analogous to
413 the chow option in our task. Unfortunately, because of our task design, it was not easy to accurately
414 identify when rats were consuming chow, and thus it was not possible to analyze neural activity
415 during chow consumption. This would be a fruitful avenue for future work. Additionally, how
416 specific is relative value coding to ACC? The orbitofrontal cortex has long been implicated in the
417 encoding of relative reward value (Tremblay & Schultz, 1999), so it would also be interesting to
418 compare signaling across frontocortical areas in future experiments.

419 **ACC inhibition versus stimulation**. If ACC activity encodes relative value signals that
420 are involved in deriving an animal's motivation to exert effort, then it is natural to predict that

disrupting ACC activity at the neural level would alter effort exertion at the behavioral level. We also expected that bidirectional manipulations of neural activity might yield bidirectional effects upon motivated effort. Indeed, impairments in effort induced by dopamine receptor blockade or dopamine depletion can be reversed by several manipulations that enhance dopamine transmission or block adenosine transmission (Farrar et al., 2010; Nunes et al., 2013; Randall et al., 2014a; Yohn et al., 2015a; Yohn et al., 2015b). Further, enhancing dopamine transmission with major psychostimulants (Yohn et al., 2016c), dopamine transporter blockers (Randall et al., 2014b; Yohn et al., 2016a), adenosine A2A receptor antagonists (Randall et al., 2012), or 5-HT2C ligands (Bailey et al., 2018; Bailey et al., 2016) can increase effort output in otherwise untreated rats.

We applied a similar rationale for our G_q and G_i DREADD experiments, and tested whether ACC chemogenetic inhibition versus stimulation yielded bidirectional effects upon behavioral responding. This was not the case: lever pressing behavior during PRC sessions was similarly attenuated by both G_q and G_i DREADDs. The contributions of ACC and other frontocortical regions to effort may be complex; for example, blocking inhibitory transmission in orbitofrontal cortex, which presumably increases local excitation, results in decreased PR responding (Munster and Hauber, 2017). Others report a similar effect of local infusion of the GABA-A antagonist bicuculline in prelimbic cortex, finding decreased high-effort choice in a two-lever operant task (Piantadosi et al., 2016). Therefore, in frontal cortex there may be an optimal excitatory/inhibitory ratio for computing relative cost-benefit and, consequently, sending appropriate output to downstream targets. It is possible that the G_q stimulation used here enhanced background noise levels in ACC, decreasing signal-to-noise ratio within the network. It is conceivable this would interfere with normal recruitment of ACC during choice lever pressing, or could even produce local inhibition *in vivo* that we were unable to detect in *ex vivo* slice recordings. The results of

444 ACC stimulation here are consistent with our manipulation introducing noise to otherwise normal
445 neural computations (Mainen and Sejnowski, 1995; Stein et al., 2005), thus impairing behavior in
446 a manner similar to when neural activity is inhibited. Lever pressing rates and neural activity levels
447 in ACC were both lower during PRC sessions than PR or CON sessions. Hence, signal-to-noise
448 ratios in ACC may have been more susceptible to interference by both excitatory and inhibitory
449 DREADDs during PRC sessions, but not during PR or CON sessions.

450 In conclusion, our findings suggest that the role of ACC in effort-based choice may be to
451 discriminate the utility of available choice options by providing a stable population code for the
452 relative value of different reward outcomes. Consequently, a disruption in decision making can
453 occur via changes in signal-to-noise ratio in this region: either by decreases in the signal (i.e. G_i
454 DREADDs), or by increases in background noise (i.e. G_q DREADDs). A better understanding of
455 ACC contributions to effort-based choice may yield insight into the mechanimsms underlying
456 motivational symptoms that occur in a wide range of conditions, particularly depression (Nunes et
457 al., 2013) and addictions (Robinson et al., 2013).

458

459 **Materials and Methods**

460 *Subjects.* Subjects were N=44 adult male Long-Evans rats (n=12 G_i DREADD experiment,
461 n=12 G_q DREADD experiment, n=10 GFP (null virus) control experiment, n=4 calcium imaging
462 experiment, n=6 acute slice recording for validation of DREADDs). Rats were obtained from
463 Charles River Laboratories (Hollister, CA), were PND 60 at the time of arrival to the UCLA
464 vivarium, and were singly-housed for all phases of experiments with the exception of the
465 acclimation period and handling, during which they were pair-housed. All rats were handled for

10 minutes in pairs for 5 d after a brief acclimation period (3 d). Rats weighed an average of 309.1 g at the beginning of experiments. Three subjects were not included in the final data analyses: one from G_i experiment and one from G_q experiment due to unilateral (not bilateral) viral expression, and one from the GCaMP experiments due to poor stability of imaging over days. Representative photomicrographs and reconstruction of DREADDs expression resulting from histological processing are shown in **Figure 1.**

The vivarium was maintained under a 12/12 h reverse light cycle at 22°C, and lab chow and water were available *ad libitum* prior to behavioral testing. Rats were food restricted one day prior to behavioral testing to ensure motivation to work for rewards. Given the sensitivity of the behavioral tests on motivation, special care was taken to maintain consistent food rations throughout the experiment. This was 12 g/d at the beginning of testing, but then decreased to 8 g/d at the beginning of the choice phase (details below). Rats were monitored every other day for their body weight, and were never permitted to drop below their 85% free feeding baseline weight. Training and testing were conducted during the early portion of the dark cycle (~0800 to 1200 H). Experiments were conducted 5-7 d per week, and rats were fed once daily on weekends (12 g) when testing was not conducted. All procedures were reviewed and approved by the Chancellor's Animal Research Committee (ARC) at the University of California, Los Angeles.

Food restriction. One day before behavioral testing began, rats were singly-housed, the amount of chow given to each rat was reduced to 12 g/d, and rats were given ~10 sucrose pellets (45-mg dustless precision sucrose pellets; Bio-Serv, Frenchtown NJ) in their home cage to acclimate them to the food rewards. Rats were maintained on 12g of food daily and were each fed within 30 min of completing the daily testing. Once rats progressed to the choice task they were

given 8 g of chow per d, in addition to the food they consumed during testing. At the time of euthanasia, rats weighed an average of 356.5 g.

Stereotaxic Surgery. General surgical procedures were the same as those recently published (Hart and Izquierdo, 2017). Rats were anesthetized with isoflurane (5% induction, 2% maintenance in 2L/min O_2). Burr holes were drilled bilaterally on the skull for insertion of 26-gauge guide cannulae (PlasticsOne, Roanoke, VA), after which 33-gauge internal cannulae (PlasticsOne, Roanoke, VA) were inserted. Rats were infused with 0.5 µL of virus at a flow rate of 0.1 µL/minute and injectors were subsequently left in place for 5 additional minutes to allow for diffusion of solution. In the G_i experiment, the virus used was AAV8-CaMKIIα-hM4D(G_i)-mCherry (Addgene, Cambridge, MA). In the G_q experiment, the virus used was AAV8-CaMKIIα-hM3D(G_q)-mCherry (Addgene, Cambridge, MA). In the GFP (null virus) control, the virus used was AAV8-CaMKIIα-eGFP (Addgene, Cambridge, MA). In the imaging experiment, the virus used was AAV9-CaMKIIα-GCaMP6f (Addgene, Cambridge, MA). The coordinates used for the guide cannulae targeting ACC (Cg1) in the G_i, G_q, and GFP control experiments were: AP= +2.0 mm, ML= ±0.7 mm, DV= −1.9 mm from Bregma. Four of twelve rats in the G_i experiment received infusions in more anterior Cg1 to compare with other laboratory experiments on decision confidence (Stolyarova et al., 2019), at AP= +3.7 mm, ML= ±0.8 mm, DV= −1.6 mm from Bregma. Since no differences emerged from this differential targeting, we combined the Cg1 groups. In the imaging experiment, coordinates were: AP= +2.0 mm, ML= ±0.7 mm, DV= −1.4 mm (0.5 µL) from Bregma, and a second 0.5 µL bolus of virus was injected at DV= -0.9 mm. Injectors extended 1 mm beyond the tip of the cannula. Following the 5-minute diffusion time, the cannulae and injectors were removed, incisions were stapled closed, and the rats were placed on a heating pad and kept in recovery until ambulatory before being returned to the vivarium.

Three days following viral infusions in the subset of rats receiving AAV9-CaMKIIα-GCaMP6f (for calcium imaging), rats were implanted with 1.8 mm diameter 0.25 pitch GRIN lenses (Edmund optics part 64-519, Barrington, NJ). Following similar surgical procedures, 4 anchor screws were secured to the skull, after which a 2.0 mm craniotomy was drilled 0.2 mm lateral to the center of the viral infusion hole. The dura was cleared and approximately 0.5 mm of tissue was aspirated, after which the lens was placed 2.0 mm ventral from the surface of the skull and secured in place with cyanoacrylate glue and bone cement. The lens was protected with Kwik-Sil (World Precision Instruments, Sarasota, FL).

Post-operative care for all rats consisted of five daily injections of carprofen (5mg/kg, s.c.) and oral sulfamethoxazole/trimethoprim solution. Two-to-three weeks following lens implantation, a small aluminum baseplate was attached to the animal's head and secured with bone cement. The exposed lens was cleaned with 100% ethanol, and the baseplate was secured in a position where cells in the field of view and vasculature were in focus. A 3D printed cover was secured to the baseplate with an anchor screw at all times when recording was not occurring. Rats were allowed a 5-d free feeding recovery period following viral infusion (G_i, G_q, and GFP experiments) or GRIN lens implantation (imaging experiment) after which they were food restricted and behavioral testing began.

Apparatus. All behavioral testing was conducted in chambers outfitted with a house light, internal stimulus lights, a food-delivery magazine, and 2 retractable levers positioned to the left and right of the chamber wall, opposite the magazine. All hardware was controlled by a PC running Med-PC IV (Med-Associates, St. Albans, VT).

Miniaturized microscope data collection. Microscopes were custom built according to plans available at Miniscope.org. Images were acquired with a CMOS imaging sensor (Labmaker,

Berlin, Germany) attached to custom data acquisition (DAQ) electronics via a 1.5 mm coaxial cable. Data were transferred to a PC running custom written DAQ software over Super Speed USB. DAQ software was written in C++ and used Open Computer Vision (OpenCV) for image acquisition. 480x752 pixel images were acquired at 30 Hz and written to .avi files. DAQ software simultaneously recorded and time-stamped behavioral data and image data, allowing for offline alignment. All hardware design files and assembly instructions are available at Miniscope.org. Calcium signals were extracted using modified constrained non-negative matrix factorization scripts in Matlab (Mathworks 2016, Natick, MA) (Pnevmatikakis et al., 2016; Zhou et al., 2018).

Lever press training. Rats were first given fixed-ratio (FR)-1 training where each lever press earned a single sucrose pellet (Bioserv, Frenchtown, NJ). They were kept on this schedule until they earned at least 30 pellets within 30 minutes. Following this, rats where shifted to a progressive ratio (PR) schedule where the required number of presses for each pellet increased according to the formula:

$$n_i = 5e^{(i/5)} - 5$$

where n_i is equal to the number of presses required on the i^{th} ratio, rounded to the nearest whole number (Richardson and Roberts, 1996), after 5 successive schedule completions. No timeout was imposed. Rats were tested on the PR schedule until they earned at least 30 pellets on any given day (~5 d) within 30 min. Upon meeting the PR performance criterion, a ceramic ramekin containing 18 g of lab chow was introduced (modified from (Randall et al., 2012)) during testing. Rats were free to choose between consuming freely-available but less preferred chow or lever pressing for preferred sucrose pellets. Rats (G_i, G_q, and GFP experiments) were given at least 5 choice testing sessions before clozapine-N-oxide (CNO) or vehicle (VEH) injections began (details below).

Drug treatment. Rats in the G_i, G_q, and GFP control experiments were given either VEH (95% saline, 5% DMSO, 1 mL/kg) or CNO (3.0 mg/kg i.p. in 95% saline, 5% DMSO, 1 mL/kg) (Tocris, Bristol, UK) 45 min prior to test sessions. Three types of test sessions were given: 1) a progressive ratio choice (PRC) session during which rats lever pressed on the PR schedule in the presence of the ceramic ramekin containing lab chow so that they were free to choose between lever pressing for sucrose versus free feeding on chow, 2) progressive ratio (PR) only sessions during which we omitted the ceramic ramekin (so that there was no freely-available lab chow) to assess whether manipulations decreased lever pressing in the absence of choice, and 3) free access to pre-weighed amounts of sucrose pellets and lab chow (18 g) in empty cages (different from their home cages). Following this, any remaining food was collected and weighed to determine rats' food preferences. All sessions were 30 min in duration. In a repeated measures design, VEH or CNO was administered prior to a PRC testing session, a PR only testing session, and a free availability choice testing session, in that order, for each rat. The order of vehicle versus CNO administration was counterbalanced for baseline choice performance. Rats were given at least 48 hours between injections, and testing never occurred on consecutive days.

Euthanasia. Following behavioral testing, rats were sacrificed by sodium pentobarbital overdose (Euthasol, 0.8 mL, 390 mg/mL pentobarbital, 50 mg/mL phenytoin; Virbac, Fort Worth, TX) and perfused transcardially with 0.9% saline followed by 10% buffered formalin acetate. Brains were post-fixed in 10% buffered formalin acetate for 24 hours followed by 30% sucrose cryoprotection for 5 days. 50 μm sections were cover slipped with DAPI mounting medium (Prolong gold, Invitrogen, Carlsbad, CA), and visualized using a BZ-X710 microscope (Keyence, Itasca, IL).

579 *DREADDs quantification.* 50 µm sections taken from each animal were visualized at seven
580 AP coordinates relative to bregma: +4.2 mm, +3.7 mm, +3.2 mm, +2.7 mm, +2.2 mm, +1.7 mm,
581 and +1.6 mm. No fluorescence was observed beyond these coordinates. mCherry fluorescence was
582 drawn by a blind experimenter on a GNU Image Manipulation Program (GIMP) document
583 containing a schematic of each of these seven sections, drawn to scale. Spread was quantified as
584 total pixel count across all seven sections.

585 *Electrophysiological confirmation of DREADDs*. Separate rats were prepared with ACC
586 (Cg1) DREADDs using identical surgical procedures to the main experiments (**Figure 2A**). Slice
587 recordings did not begin until at least four weeks following surgery to allow sufficient hM receptor
588 expression. Slice recording methods were similar to those previously published (Babiec et al.,
589 2017). Six rats were deeply anesthetized with isoflurane and decapitated. The brain was rapidly
590 removed and submerged in ice-cold, oxygenated (95% O_2/5% CO_2) artificial cerebrospinal fluid
591 (ACSF) containing (in mM) as follows: 124 NaCl, 4 KCl, 25 $NaHCO_3$, 1 NaH_2PO_4, 2 $CaCl_2$, 1.2
592 $MgSO_4$, and 10 glucose (Sigma-Aldrich). 400-µm-thick slices containing the ACC were then cut
593 using a Campden 7000SMZ-2 vibratome. Slices from the site of viral infusion were used for
594 validation. Expression of mCherry was confirmed after recordings were performed, and ACC
595 slices with no transfection were used as control slices. Slices were maintained (at 30°C) in
596 interface-type chambers that were continuously perfused (2–3 ml/min) with ACSF and allowed to
597 recover for at least 2 hours before recordings. Following recovery, slices were perfused in a
598 submerged-slice recording chamber (2–3 ml/min) with ACSF containing 100 µM picrotoxin to
599 block $GABA_A$ receptor-mediated inhibitory synaptic currents. A glass microelectrode filled with
600 ACSF (resistance = 5–10 MΩ) was placed in layer 2/3 ACC to record field excitatory postsynaptic
601 synaptic potentials and postsynaptic responses elicited by layer 1 stimulation delivered using a

bipolar, nichrome-wire stimulating electrode placed near the medial wall in ACC. Inhibitory validation in ACC with identical coordinates, reagents, and virus was previously performed by our lab, with the methods and data appearing elsewhere (Stolyarova et al., 2019) and so these experiments were not needlessly repeated. Briefly, we first recorded for 2 minutes without synaptic stimulation to measure spontaneous levels of activity. Presynaptic fiber stimulation (0.2 msec duration pulses delivered at 0.33 Hz) was then delivered and the stimulation intensity was varied in 0.2 V increments to generate an input/output curve and identify the threshold for generation of postsynaptic responses. Stimulation strength was then set to the minimum level required to induce postsynaptic responses in ACC. Once stable responses (measured as the area of responses over a 4 second interval) were detected, baseline measures were taken for at least 10 minutes, followed by 20 minutes bath application of 10 μM CNO. In slices where CNO failed to elicit spontaneous activity, we generated a second input/output in the presence of CNO to test for CNO-induced changes in postsynaptic responses evoked by synaptic stimulation. Unless noted otherwise, all chemicals were obtained from Sigma-Aldrich.

Behavioral analyses. Behavioral data were analyzed using GraphPad Prism v.7 (La Jolla, CA) and SPSS v.25 (Armonk, NY). An alpha level for significance was set to 0.05. Paired samples t-tests (reported as means ± SEM) on data from the choice and PR-only tests were used to test for effects of CNO. Two-way ANOVA was used to test for effects of CNO on food preference in the free choice test.

Calcium image analyses. Image analyses were performed using custom written MATLAB scripts. First, images were motion corrected using functions based on the Non-Rigid Motion Correction ("NoRMCorre") package (Pnevmatikakis and Giovannucci, 2017), downsampled spatially by a factor of two (240x356 pixels) and temporally by a factor of 4 (to a frame rate of 7.5

fps). In order to remove background fluorescence, we performed a neural enhancement processing step as in the min1pipe processing framework (Lu et al., 2018). Briefly, from each frame we constructed a background fluorescence estimate by performing a neuron-sized morphological opening function, and subtracting this background frame from the original frame. This removes large fluorescence artifacts inherent in single photon microscopy, while preserving neural components. This motion corrected, downsampled, and enhanced video was then processed using Constrained Non-negative Matrix Factorization for Endoscopic data, "CNMF-E", (Pnevmatikakis et al., 2016; Zhou et al., 2018). This extracted individual neural segments, denoised their fluorescent signals, demixed cross-talk from nearby neighbors, and deconvolved the calcium transients in order to estimate instances of increased firing activity for each neuron. These estimated spike timings were used to compare neural firing time-locked to specific behavioral instances. Neurons were matched across recording sessions using CellReg (Sheintuch et al., 2017) by matching cells based on their contours and centroid locations.

Imaging behavioral analysis. For each recording session, we identified every bout of lever pressing (LP) or sucrose magazine head entry (HE). We computed baseline calcium transient probabilities for each cell from time periods not surrounding LPs and HEs ($\pm$5 seconds). Around the beginning of each LP and HE bout we created 6 second ($\pm$3) peri-event time histograms (PETHs) on the inferred spike times for every cell recorded within a session, yielding an average calcium transient rate per bin. We then compared each time bin to the cell's baseline transient probability with a binomial test to evaluate significantly modulated time bins surrounding either LPs or HEs. Cells with at least 3 bins with probability <= .01 were deemed significantly responsive to either behavior. To compare cell responses to LPs or HEs across different session types, we selected cells that were 1) significanty modulated in at least 1 of any session type and 2) was

detected in at least 1 session of each type (regardless of significance). PETHs for each cell were averaged across sessions of the same type, and the peak response time was determined from the max time bin of the gaussian smoothed average PETH (3 bin width, 400ms). Cells were split into pre- and post-bout labels based on their summed response magnitude before and after LP or HE (pre: <0, post: >0). Cells with a pre-LP response in either PR, PRC, or CON conditions, and were detected in every condition, were labelled as "pre-LP" cells (**Figure 7A**). Cells with a post-HE response in either PR, PRC, or CON conditions, and were detected in every condition, were labelled as "post-HE" cells (**Figure 7D**). Cells that fell into the post-LP and pre-HE category were not evaluated due to the substantial overlap between behaviors during this time period. The average PETH of the pre-LP and post-HE populations were constructed to yield population response curves (**Figure 7B,E**). Pre-LP cells were evaluated across the three conditions using the average response for each cell during the pre-lever-press time bins (<0 sec) and post HE cells were evaluated using the average response per cell after head-entry (>0 sec) (**Figure 7C,F**).

Satiety Control Condition. For a subset of calcium imaging sessions, we administered a satiety control condition. For these sessions we capitalized on the fact that rats typically consume chow early in the test session, presented them with the lever and the chow initially, allowed them to consume chow, but then removed the chow once the rat began to lever press. This control condition allowed rats to reach a comparable motivational (more sated) state relative to the PR-only condition, and thus controlled for satiety differences between PR and PRC sessions.

Acknowledgements: This work was supported by UCLA's Division of Life Sciences Recruitment and Retention fund (Izquierdo), R01 DA047870 (Izquierdo), NSF Neuronex 170748 (Blair), the Training program in Translational Neuroscience of Drug Abuse (T32 DA024635, London), and the Training program in Neural Microcircuits (T32 NS058280, Feldman). We thank members of the Izquierdo lab for helpful comments on a previous version of the manuscript. We acknowledge the Staglin Center for Brain

674 and Behavioral Health for additional support related to fluorescence microscopy and UCLA Graduate
675 Division for the Dissertation Year Fellowship (Hart).
676
677 **Conflict of Interest:** The authors declare no competing financial interests
678

Supplementary Figures

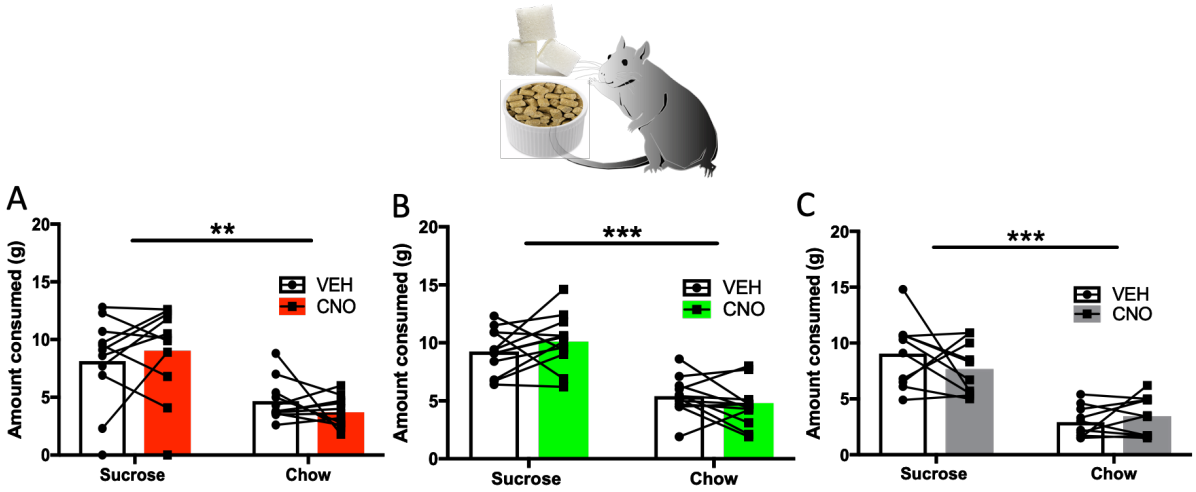

Supplementary Figure 1. Free choice behavior in all three treatment groups following CNO administration. Mean consumption of sucrose and chow when rats were presented with both as freely-available options. Shown is within-subject, counterbalanced choice behavior under vehicle and CNO, indicating that food preference was intact: rats preferred the sucrose over chow. **(A)** CNO had no effect on either sucrose or chow consumed in the G_i DREADDs condition. **(B)** CNO had no effect on either sucrose or chow consumed in the G_q DREADDs condition. **(C)** CNO had no effect on either sucrose or chow consumed in the null virus (GFP) condition. **p<0.01, ***p<0.001.

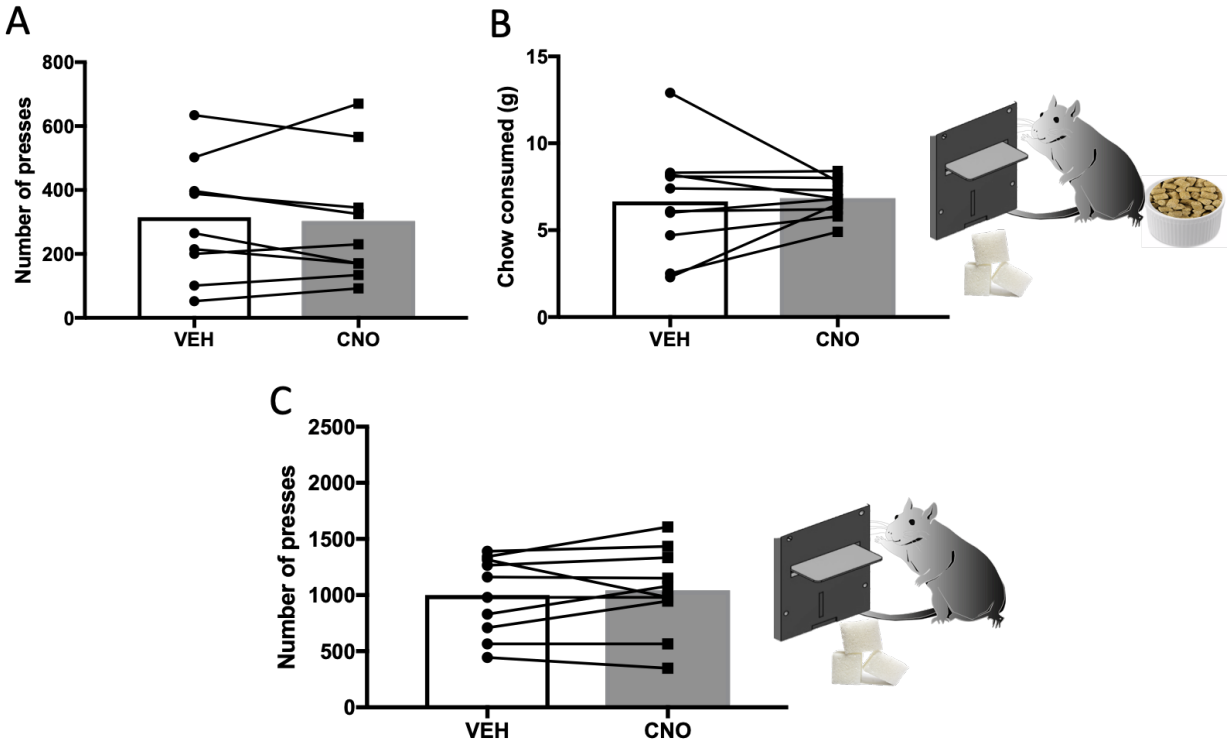

Supplementary Figure 2. No effect on effortful choice behavior following CNO administration in GFP (null virus) controls. Shown is within-subject measures under counterbalanced conditions of vehicle and CNO in null virus controls. **(A)** Mean total lever presses during PRC sessions, when rats were presented with both the possibility of lever pressing under a PR schedule for sucrose pellets and freely-available chow. Unlike following active virus, CNO had no significant effect on the number of lever presses in this condition. **(B)** Total chow consumed during choice testing was also not different between vehicle and CNO conditions. **(C)** Mean lever presses during PR testing when there was no chow available as an alternative option. Lever pressing was also not different between vehicle and CNO conditions.

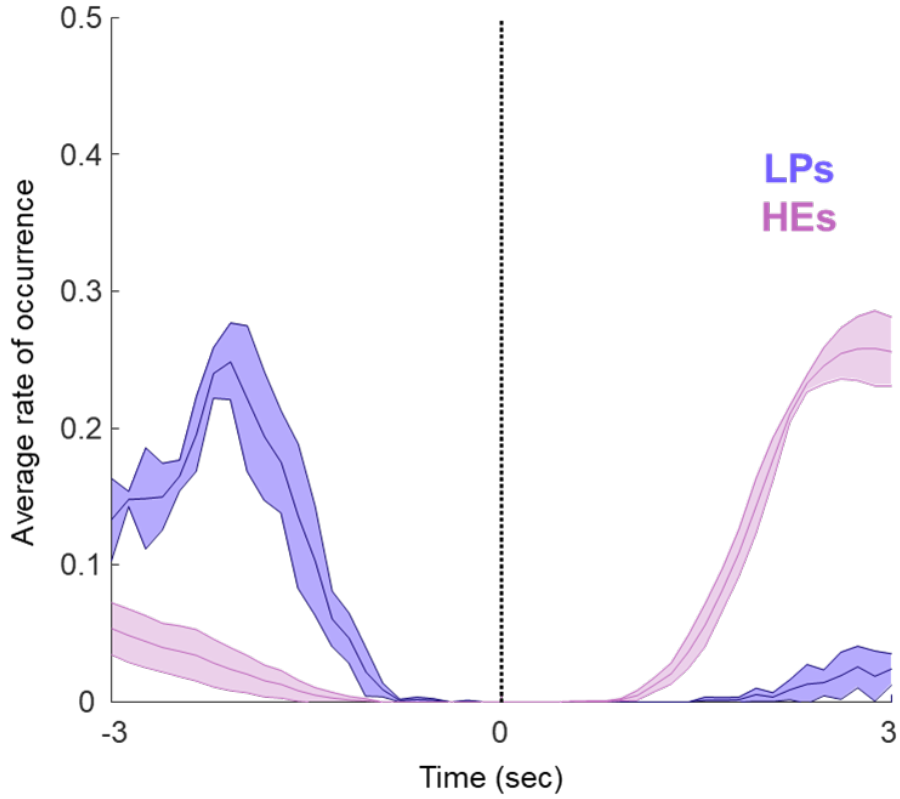

Supplementary Figure 3. Behavior triggered behavior PETH demonstrating behavioral overlap in post-LP and pre-HE periods. Histogram of lever-presses based on head-entries (blue). Histogram of Head-entries based on lever-presses (magenta). The 3 second time window following LPs and preceding HEs show substantial contamination from the other behavior, and were thus excluded from our analysis.

References

Akam, T., Rodrigues-Vaz, I., Zhang, X., Pereira, M., Oliveira, R., Dayan, P., and Costa, R.M. (2017). Single-Trial Inhibition of Anterior Cingulate Disrupts Model-based Reinforcement Learning in a Two-step Decision Task. bioRxiv, 126292.

Azab, H., and Hayden, B.Y. (2017). Correlates of decisional dynamics in the dorsal anterior cingulate cortex. PLoS Biol *15*, e2003091.

Babiec, W.E., Jami, S.A., Guglietta, R., Chen, P.B., and O'Dell, T.J. (2017). Differential Regulation of NMDA Receptor-Mediated Transmission by SK Channels Underlies Dorsal-Ventral Differences in Dynamics of Schaffer Collateral Synaptic Function. J Neurosci *37*, 1950-1964.

Bailey, M.R., Goldman, O., Bello, E.P., Chohan, M.O., Jeong, N., Winiger, V., Chun, E., Schipani, E., Kalmbach, A., Cheer, J.F., *et al.* (2018). An Interaction between Serotonin Receptor Signaling and Dopamine Enhances Goal-Directed Vigor and Persistence in Mice. J Neurosci *38*, 2149-2162.

Bailey, M.R., Williamson, C., Mezias, C., Winiger, V., Silver, R., Balsam, P.D., and Simpson, E.H. (2016). The effects of pharmacological modulation of the serotonin 2C receptor on goal-directed behavior in mice. Psychopharmacology (Berl) *233*, 615-624.

Bernacchia, A., Seo, H., Lee, D., and Wang, X.J. (2011). A reservoir of time constants for memory traces in cortical neurons. Nat Neurosci *14*, 366-372.

Blanchard, T.C., and Hayden, B.Y. (2014). Neurons in dorsal anterior cingulate cortex signal postdecisional variables in a foraging task. J Neurosci *34*, 646-655.

Cousins, M.S., Atherton, A., Turner, L., and Salamone, J.D. (1996). Nucleus accumbens dopamine depletions alter relative response allocation in a T-maze cost/benefit task. Behav Brain Res *74*, 189-197.

Cousins, M.S., and Salamone, J.D. (1994). Nucleus accumbens dopamine depletions in rats affect relative response allocation in a novel cost/benefit procedure. Pharmacol Biochem Behav *49*, 85-91.

Cowen, S.L., Davis, G.A., and Nitz, D.A. (2012). Anterior cingulate neurons in the rat map anticipated effort and reward to their associated action sequences. J Neurophysiol *107*, 2393-2407.

Farrar, A.M., Segovia, K.N., Randall, P.A., Nunes, E.J., Collins, L.E., Stopper, C.M., Port, R.G., Hockemeyer, J., Muller, C.E., Correa, M., *et al.* (2010). Nucleus accumbens and effort-related functions: behavioral and neural markers of the interactions between adenosine A2A and dopamine D2 receptors. Neuroscience *166*, 1056-1067.

Floresco, S.B., and Ghods-Sharifi, S. (2007). Amygdala-prefrontal cortical circuitry regulates effort-based decision making. Cereb Cortex *17*, 251-260.

766 Gabbott, P.L., Warner, T.A., Jays, P.R., Salway, P., and Busby, S.J. (2005). Prefrontal cortex in
767 the rat: projections to subcortical autonomic, motor, and limbic centers. J Comp Neurol *492*, 145-177.
768 Ghods-Sharifi, S., and Floresco, S.B. (2010). Differential effects on effort discounting induced by
769 inactivations of the nucleus accumbens core or shell. Behav Neurosci *124*, 179-191.
770 Hart, E.E., Gerson, J.O., and Izquierdo, A. (2018). Persistent effect of withdrawal from
771 intravenous methamphetamine self-administration on brain activation and behavioral economic indices
772 involving an effort cost. Neuropharmacology *140*, 130-138.
773 Hart, E.E., Gerson, J.O., Zoken, Y., Garcia, M., and Izquierdo, A. (2017). Anterior cingulate
774 cortex supports effort allocation towards a qualitatively preferred option. Eur J Neurosci *46*, 1682-1688.
775 Hart, E.E., and Izquierdo, A. (2017). Basolateral amygdala supports the maintenance of value and
776 effortful choice of a preferred option. Eur J Neurosci *45*, 388-397.
777 Hart, E.E., and Izquierdo, A. (2019). Quantity versus quality: Convergent findings in effort-based
778 choice tasks. Behav Processes *164*, 178-185.
779 Hauber, W., and Sommer, S. (2009). Prefrontostriatal circuitry regulates effort-related decision
780 making. Cereb Cortex *19*, 2240-2247.
781 Hayden, B.Y., Pearson, J.M., and Platt, M.L. (2009). Fictive reward signals in the anterior
782 cingulate cortex. Science *324*, 948-950.
783 Hayden, B.Y., Pearson, J.M., and Platt, M.L. (2011). Neuronal basis of sequential foraging
784 decisions in a patchy environment. Nat Neurosci *14*, 933-939.
785 Heilbronner, S.R., and Hayden, B.Y. (2016). Dorsal Anterior Cingulate Cortex: A Bottom-Up
786 View. Annu Rev Neurosci *39*, 149-170.
787 Hillman, K.L., and Bilkey, D.K. (2010). Neurons in the rat anterior cingulate cortex dynamically
788 encode cost-benefit in a spatial decision-making task. J Neurosci *30*, 7705-7713.
789 Hillman, K.L., and Bilkey, D.K. (2012). Neural encoding of competitive effort in the anterior
790 cingulate cortex. Nat Neurosci *15*, 1290-1297.
791 Hosking, J.G., Cocker, P.J., and Winstanley, C.A. (2014). Dissociable contributions of anterior
792 cingulate cortex and basolateral amygdala on a rodent cost/benefit decision-making task of cognitive
793 effort. Neuropsychopharmacology *39*, 1558-1567.
794 Hunt, L.T., and Hayden, B.Y. (2017). A distributed, hierarchical and recurrent framework for
795 reward-based choice. Nat Rev Neurosci *18*, 172-182.
796 Hyman, J.M., Holroyd, C.B., and Seamans, J.K. (2017). A Novel Neural Prediction Error Found
797 in Anterior Cingulate Cortex Ensembles. Neuron *95*, 447-456 e443.
798 Kennerley, S.W., Behrens, T.E., and Wallis, J.D. (2011). Double dissociation of value
799 computations in orbitofrontal and anterior cingulate neurons. Nat Neurosci *14*, 1581-1589.

Lapish, C.C., Durstewitz, D., Chandler, L.J., and Seamans, J.K. (2008). Successful choice behavior is associated with distinct and coherent network states in anterior cingulate cortex. Proc Natl Acad Sci U S A *105*, 11963-11968.

Lu, J., Li, C., Singh-Alvarado, J., Zhou, Z.C., Frohlich, F., Mooney, R., and Wang, F. (2018). MIN1PIPE: A Miniscope 1-Photon-Based Calcium Imaging Signal Extraction Pipeline. Cell Rep *23*, 3673-3684.

Mainen, Z.F., and Sejnowski, T.J. (1995). Reliability of spike timing in neocortical neurons. Science *268*, 1503-1506.

Mashhoori, A., Hashemnia, S., McNaughton, B.L., Euston, D.R., and Gruber, A.J. (2018). Rat anterior cingulate cortex recalls features of remote reward locations after disfavoured reinforcements. Elife *7*.

Munster, A., and Hauber, W. (2017). Medial Orbitofrontal Cortex Mediates Effort-related Responding in Rats. Cereb Cortex, 1-11.

Nathanson, J.L., Yanagawa, Y., Obata, K., and Callaway, E.M. (2009). Preferential labeling of inhibitory and excitatory cortical neurons by endogenous tropism of adeno-associated virus and lentivirus vectors. Neuroscience *161*, 441-450.

Nowend, K.L., Arizzi, M., Carlson, B.B., and Salamone, J.D. (2001). D1 or D2 antagonism in nucleus accumbens core or dorsomedial shell suppresses lever pressing for food but leads to compensatory increases in chow consumption. Pharmacol Biochem Behav *69*, 373-382.

Nunes, E.J., Randall, P.A., Hart, E.E., Freeland, C., Yohn, S.E., Baqi, Y., Muller, C.E., Lopez-Cruz, L., Correa, M., and Salamone, J.D. (2013). Effort-related motivational effects of the VMAT-2 inhibitor tetrabenazine: implications for animal models of the motivational symptoms of depression. J Neurosci *33*, 19120-19130.

Piantadosi, P.T., Khayambashi, S., Schluter, M.G., Kutarna, A., and Floresco, S.B. (2016). Perturbations in reward-related decision-making induced by reduced prefrontal cortical GABA transmission: Relevance for psychiatric disorders. Neuropharmacology *101*, 279-290.

Pnevmatikakis, E.A., and Giovannucci, A. (2017). NoRMCorre: An online algorithm for piecewise rigid motion correction of calcium imaging data. J Neurosci Methods *291*, 83-94.

Pnevmatikakis, E.A., Soudry, D., Gao, Y., Machado, T.A., Merel, J., Pfau, D., Reardon, T., Mu, Y., Lacefield, C., Yang, W.*, et al.* (2016). Simultaneous Denoising, Deconvolution, and Demixing of Calcium Imaging Data. Neuron *89*, 285-299.

Porter, B.S., Hillman, K.L., and Bilkey, D.K. (2019). Anterior cingulate cortex encoding of effortful behavior. J Neurophysiol *121*, 701-714.

Procyk, E., Tanaka, Y.L., and Joseph, J.P. (2000). Anterior cingulate activity during routine and non-routine sequential behaviors in macaques. Nat Neurosci *3*, 502-508.

Randall, P.A., Lee, C.A., Nunes, E.J., Yohn, S.E., Nowak, V., Khan, B., Shah, P., Pandit, S., Vemuri, V.K., Makriyannis, A.*, et al.* (2014a). The VMAT-2 inhibitor tetrabenazine affects effort-related decision making in a progressive ratio/chow feeding choice task: reversal with antidepressant drugs. PLoS One *9*, e99320.

Randall, P.A., Lee, C.A., Podurgiel, S.J., Hart, E., Yohn, S.E., Jones, M., Rowland, M., Lopez-Cruz, L., Correa, M., and Salamone, J.D. (2014b). Bupropion increases selection of high effort activity in rats tested on a progressive ratio/chow feeding choice procedure: implications for treatment of effort-related motivational symptoms. Int J Neuropsychopharmacol *18*.

Randall, P.A., Lee, C.A., Podurgiel, S.J., Hart, E., Yohn, S.E., Jones, M., Rowland, M., Lopez-Cruz, L., Correa, M., and Salamone, J.D. (2015). Bupropion increases selection of high effort activity in rats tested on a progressive ratio/chow feeding choice procedure: implications for treatment of effort-related motivational symptoms. Int J Neuropsychopharmacol *18*.

Randall, P.A., Pardo, M., Nunes, E.J., Lopez Cruz, L., Vemuri, V.K., Makriyannis, A., Baqi, Y., Muller, C.E., Correa, M., and Salamone, J.D. (2012). Dopaminergic modulation of effort-related choice behavior as assessed by a progressive ratio chow feeding choice task: pharmacological studies and the role of individual differences. PLoS One *7*, e47934.

Richardson, N.R., and Roberts, D.C. (1996). Progressive ratio schedules in drug self-administration studies in rats: a method to evaluate reinforcing efficacy. J Neurosci Methods *66*, 1-11.

Robinson, M.J., Robinson, T.E., and Berridge, K.C. (2013). Incentive salience and the transition to addiction. Biological Research on Addiction *2*, 391-399.

Salamone, J.D., Correa, M., Farrar, A., and Mingote, S.M. (2007). Effort-related functions of nucleus accumbens dopamine and associated forebrain circuits. Psychopharmacology (Berl) *191*, 461-482.

Salamone, J.D., Correa, M., Mingote, S., and Weber, S.M. (2003). Nucleus accumbens dopamine and the regulation of effort in food-seeking behavior: implications for studies of natural motivation, psychiatry, and drug abuse. J Pharmacol Exp Ther *305*, 1-8.

Salamone, J.D., Correa, M., Yang, J.H., Rotolo, R., and Presby, R. (2018). Dopamine, Effort-Based Choice, and Behavioral Economics: Basic and Translational Research. Front Behav Neurosci *12*, 52.

Salamone, J.D., Correa, M., Yohn, S.E., Yang, J.-H., Somerville, M., Rotolo, R.A., and Presby, R.E. (2017). Behavioral activation, effort-based choice, and elasticity of demand for motivational stimuli: Basic and translational neuroscience approaches. Motivation Science *3*, 208-229.

Salamone, J.D., Cousins, M.S., and Bucher, S. (1994). Anhedonia or anergia? Effects of haloperidol and nucleus accumbens dopamine depletion on instrumental response selection in a T-maze cost/benefit procedure. Behav Brain Res *65*, 221-229.

Salamone, J.D., Steinpreis, R.E., McCullough, L.D., Smith, P., Grebel, D., and Mahan, K. (1991). Haloperidol and nucleus accumbens dopamine depletion suppress lever pressing for food but increase free food consumption in a novel food choice procedure. Psychopharmacology (Berl) *104*, 515-521.

Schweimer, J., and Hauber, W. (2005). Involvement of the rat anterior cingulate cortex in control of instrumental responses guided by reward expectancy. Learn Mem *12*, 334-342.

Schweimer, J., and Hauber, W. (2006). Dopamine D1 receptors in the anterior cingulate cortex regulate effort-based decision making. Learn Mem *13*, 777-782.

Seo, H., and Lee, D. (2007). Temporal filtering of reward signals in the dorsal anterior cingulate cortex during a mixed-strategy game. J Neurosci *27*, 8366-8377.

Sheintuch, L., Rubin, A., Brande-Eilat, N., Geva, N., Sadeh, N., Pinchasof, O., and Ziv, Y. (2017). Tracking the Same Neurons across Multiple Days in Ca(2+) Imaging Data. Cell Rep *21*, 1102-1115.

Shenhav, A., Botvinick, M.M., and Cohen, J.D. (2013). The expected value of control: an integrative theory of anterior cingulate cortex function. Neuron *79*, 217-240.

Shidara, M., and Richmond, B.J. (2002). Anterior cingulate: single neuronal signals related to degree of reward expectancy. Science *296*, 1709-1711.

Skvortsova, V., Palminteri, S., and Pessiglione, M. (2014). Learning to minimize efforts versus maximizing rewards: computational principles and neural correlates. J Neurosci *34*, 15621-15630.

Stein, R.B., Gossen, E.R., and Jones, K.E. (2005). Neuronal variability: noise or part of the signal? Nat Rev Neurosci *6*, 389-397.

Stolyarova, A., Rakhshan, M., Hart, E.E., O'Dell, T.J., Peters, M., Lau, H., Soltani, A., and Izquierdo, A. (2019). Dissociable roles for Anterior Cingulate Cortex and Basolateral Amygdala in Decision Confidence and Learning under Uncertainty. bioRxiv, 655860.

Thompson, A.B., Gerson, J., Stolyarova, A., Bugarin, A., Hart, E.E., Jentsch, J.D., and Izquierdo, A. (2017). Steep effort discounting of a preferred reward over a freely-available option in prolonged methamphetamine withdrawal in male rats. Psychopharmacology (Berl) *234*, 2697-2705.

Tremblay, L., and Schultz, W. (1999). Relative reward preference in primate orbitofrontal cortex. Nature 398, 704-708.

Vogt, B.A., and Paxinos, G. (2014). Cytoarchitecture of mouse and rat cingulate cortex with human homologies. Brain Struct Funct *219*, 185-192.

900 Walton, M.E., Bannerman, D.M., Alterescu, K., and Rushworth, M.F. (2003). Functional
901 specialization within medial frontal cortex of the anterior cingulate for evaluating effort-related decisions.
902 J Neurosci *23*, 6475-6479.
903 Walton, M.E., Bannerman, D.M., and Rushworth, M.F. (2002). The role of rat medial frontal
904 cortex in effort-based decision making. J Neurosci *22*, 10996-11003.
905 Wang, X., Zhang, C., Szabo, G., and Sun, Q.Q. (2013). Distribution of CaMKIIalpha expression
906 in the brain in vivo, studied by CaMKIIalpha-GFP mice. Brain Res *1518*, 9-25.
907 Winstanley, C.A., and Floresco, S.B. (2016). Deciphering Decision Making: Variation in Animal
908 Models of Effort- and Uncertainty-Based Choice Reveals Distinct Neural Circuitries Underlying Core
909 Cognitive Processes. J Neurosci *36*, 12069-12079.
910 Yohn, S.E., Errante, E.E., Rosenbloom-Snow, A., Somerville, M., Rowland, M., Tokarski, K.,
911 Zafar, N., Correa, M., and Salamone, J.D. (2016a). Blockade of uptake for dopamine, but not
912 norepinephrine or 5-HT, increases selection of high effort instrumental activity: Implications for
913 treatment of effort-related motivational symptoms in psychopathology. Neuropharmacology *109*, 270-
914 280.
915 Yohn, S.E., Gogoj, A., Haque, A., Lopez-Cruz, L., Haley, A., Huxley, P., Baskin, P., Correa, M.,
916 and Salamone, J.D. (2016b). Evaluation of the effort-related motivational effects of the novel dopamine
917 uptake inhibitor PRX-14040. Pharmacol Biochem Behav *148*, 84-91.
918 Yohn, S.E., Lopez-Cruz, L., Hutson, P.H., Correa, M., and Salamone, J.D. (2016c). Effects of
919 lisdexamfetamine and s-citalopram, alone and in combination, on effort-related choice behavior in the rat.
920 Psychopharmacology (Berl) *233*, 949-960.
921 Yohn, S.E., Santerre, J.L., Nunes, E.J., Kozak, R., Podurgiel, S.J., Correa, M., and Salamone, J.D.
922 (2015a). The role of dopamine D1 receptor transmission in effort-related choice behavior: Effects of D1
923 agonists. Pharmacol Biochem Behav *135*, 217-226.
924 Yohn, S.E., Thompson, C., Randall, P.A., Lee, C.A., Muller, C.E., Baqi, Y., Correa, M., and
925 Salamone, J.D. (2015b). The VMAT-2 inhibitor tetrabenazine alters effort-related decision making as
926 measured by the T-maze barrier choice task: reversal with the adenosine A2A antagonist MSX-3 and the
927 catecholamine uptake blocker bupropion. Psychopharmacology (Berl) *232*, 1313-1323.
928 Zhou, P., Resendez, S.L., Rodriguez-Romaguera, J., Jimenez, J.C., Neufeld, S.Q., Giovannucci,
929 A., Friedrich, J., Pnevmatikakis, E.A., Stuber, G.D., Hen, R.*, et al.* (2018). Efficient and accurate
930 extraction of in vivo calcium signals from microendoscopic video data. Elife *7*.

931